MAIN ARTICLE

Application of a variance-based sensitivity analysis method to the Biomass Scenario Learning Model

Paige Jadun,* Laura J. Vimmerstedt, Brian W. Bush, Daniel Inman and Steve Peterson

Abstract

Variance-based sensitivity analysis can provide a comprehensive understanding of the input factors that drive model behavior, complementing more traditional system dynamics methods with quantitative metrics. This paper presents the methodology of a variance-based sensitivity analysis of the Biomass Scenario Learning Model, a published STELLA model of interactions among investment, production, and learning in an emerging competitive industry. We document the methodology requirements, interpretations, and constraints, and compute estimated sensitivity indices and their uncertainties. We show that application of variance-based sensitivity analysis to the model allows us to test for non-additivity, identify influential and interactive variables, and confirm model formulation. To enable use of this type of sensitivity analysis in other system dynamics models, we provide this study's R code, annotated to facilitate adaptation to other studies. A related paper describes application of these techniques to the much larger Biomass Scenario Model.

Syst. Dyn. Rev. **33**, 311–335 (2017)

Additional Supporting Information may be found online in the supporting information tab for this article.

Introduction

The Biomass Scenario Model (BSM) is a system dynamics model of the biomass to biofuels supply chain, written in STELLA (isee systems, 2014). Together with the U.S. Department of Energy (DOE), the National Renewable Energy Laboratory (NREL) developed the BSM to explore scenarios for development of the biofuels industry. The BSM incorporates thousands of input values which, due to the presence of myriad feedback dynamics and

National Renewable Energy Laboratory, 15013 Denver West Parkway, Golden, CO, 80401, U.S.A.
* Correspondence to: Paige Jadun. E-mail: paige.jadun@nrel.gov

Accepted by Andreas Größler, Received 15 December 2016; Revised 9 August 2017; 1 September 2017; 5 April 2018 and 17 May 2018; Accepted 18 May 2018

System Dynamics Review
System Dynamics Review vol 33, No 3-4 (July-December 2017): 311–335
Published online in Wiley Online Library
(wileyonlinelibrary.com) DOI: 10.1002/sdr.1594

relationships in the model, have the potential to result in complex and nonlinear behaviors (Peterson *et al.*, 2013). Variance in the inputs, coupled with the potential for interactions among inputs, complicates interpretation of the model output. Understanding how these complex interactions drive model behavior is pivotal to interpreting model results, highlighting the need for comprehensive analysis methods. This paper aims to address that need by presenting the application of variance-based sensitivity analysis methods to part of the BSM.

For the purposes of this study, a smaller, simpler extract of the BSM, called the biomass learning model, was selected for sensitivity analysis (Vimmerstedt *et al.* 2015). The Learning Model represents the industrial learning process for three illustrative biofuel industries and is designed to elucidate the impact that certain learning inputs have on the overall biofuels industrial output (i.e. fuel production). By extracting the Learning Model from the rest of the supply chain in the full BSM, we focus on the industrial learning process, a key factor in the growth of many new industries, such as the biofuels industry. Understanding and quantifying influential factors for total industrial output across a broad range of input conditions necessitates a statistically rigorous experimental design and analysis.

Sensitivity analysis is the assessment of how uncertainty in a model's output can be apportioned to uncertainty in the model's input factors (Saltelli *et al.*, 2010). For a forward-looking simulation model such as the BSM, most of the input assumptions about the future cannot be statistically estimated from historical data, but instead are taken from published literature or process knowledge (Lin *et al.*, 2013). Sensitivity analysis methods allow for the exploration of model behavior across a broad range of conditions. Especially with large and complex models, exploring the full range of input space manually can be cumbersome and time prohibitive. Quantitative sensitivity analysis methods, such as those described in this paper, can complement traditional methods used in the system dynamics community by providing a more thorough understanding of model behaviors.

Categories of sensitivity analysis include factor prioritization, factor fixing, factor mapping, and metamodeling. Saltelli *et al.* (2004) detail each of these methods, and Pianosi *et al.* (2016) provide a comparative review. Sterman (2000) describes best- and worst-case scenarios, Monte Carlo simulations, and automated nonlinear tests as methods for sensitivity analysis. These methods help in understanding the bounds of model behavior (best- and worst-case scenarios), likely outcomes (Monte Carlo simulations), and the search for anomalous results (automated nonlinear tests) (Sterman, 2000). In this study, we employ a factor-fixing approach. Factor-fixing approaches identify which factors, among all model factors, can be fixed (i.e. assigned any value within its range) without any appreciable impact on the model's output. This is in contrast to factor prioritization approaches, including elementary effects (Morris 1991), which identify potentially important factors,

DOI: 10.1002/sdr

and factor-mapping approaches, such as Monte Carlo filtering (Saltelli *et al.*, 2008), which are used to find which factors produce model results in a particular output space.

Various sensitivity analysis approaches have been applied to systems dynamics models. The literature reports on numerical sensitivity analysis of model parameters, which is considered in this study, in addition to analysis of the sensitivity of models to graphical functions (Eker *et al.*, 2014) and the sensitivity of model behavior patterns to changes in model parameters (Hekimoğlu and Barlas, 2016; Walgrave, 2016). Literature on numerical sensitivity analysis of model parameters includes application and review of several statistical methods (Bier, 2011), the use of regression and design of experiments (Kleijnen, 1995), the use of statistical screening methods (Ford and Flynn, 2005) for factor prioritization (Taylor *et al.*, 2010), and together with design of experiments (Jalili and Ford, 2016). This analysis contributes to the literature by presenting a case study on the application of variance decomposition-based sensitivity of a system dynamic model. We use nonparametric methods to analyze the results from this study and demonstrate the power of this approach to rapidly develop model intuition from system dynamic models.

For this study, we developed an approach to apply Sobol's variance-based sensitivity method (Sobol, 1993) to the BSM. This method has many desirable features, such as independence in the estimates of sensitivity indices (i.e. potential non-additivity in the model does not affect its sensitivity index), and the ability to assess a very broad range of input settings (Saltelli *et al.*, 2010). More importantly, this methodology allows for the quantification of interaction effects in model behavior, which may be more difficult to uncover with other methods of model exploration described above. For variance-based sensitivity analysis, a systematic methodology involves identifying the factors of interest and their ranges, choosing a sample size and sampling approach, and deciding on which indices to compute.

The simpler Learning Model is used in this study to develop a clear methodology for variance-based sensitivity analysis of a systems dynamics model in a context that can be easily understood. The goal of this paper is to document the application of Sobol's method to the biomass learning model, including the method requirements, interpretations, and constraints. As a result of the analysis, we compute estimated sensitivity indices and their uncertainties. Application of the methods developed in this study to the more complex BSM is the subject of analysis by Inman *et al.* (2018), which focuses on the resulting insights into model behavior and their significance to the biofuels industry.

DOI: 10.1002/sdr

Biomass learning model

This paper focuses on the biomass learning model, a part of the BSM that is extracted from the larger model. The Learning Model provides a simpler context for exploration. Instead of the full set of actual pathways, the Learning Model includes only three competing biofuel conversion pathways—generically characterized and named A, B, and C—as they develop through three stages (pilot, demonstration, and commercial). The biomass learning model simulates the interplay among technological improvement, investment, and commercial production in an emerging industry. Vimmerstedt *et al.* (2015) document the biomass learning model, which is available at https://github.com/NREL/bsm-learning.

The primary dynamic feature in the biomass learning model is based on the concept of the learning curve. In the energy sector, a single-factor learning curve is often used, in which the percentage decrease in unit costs is a function of a single factor, the doubling of industrial experience, usually expressed as cumulative production (Eq. (1)) (Vimmerstedt *et al.*, 2015):

$$Y = aX^b \tag{1}$$

where Y is the current unit cost, X is the cumulative production, a is the unit cost of the initial unit, b is the slope of the function when plotted on a log–log scale, and PR is the progress ratio:

$$\mathrm{PR} = 2^{-b} \tag{2}$$

The literature on learning curves generally estimates a historical progress ratio (Eq. (2)), which may be used to extrapolate technological improvement into the future (Vimmerstedt *et al.*, 2015). The progress ratio represents the relative cost after each doubling of cumulative production; a lower progress ratio results in faster learning. The sensitivity analysis detailed in this paper focuses on the influence of progress ratios of the three competing biofuel conversion pathways on the total industrial output in the biomass learning model.

A stock–flow diagram that encompasses the major dynamics of the biomass learning model is shown in Figure 1. The top row, with stocks measured in number of biorefineries, shows Initiating biorefineries flowing into biorefineries In Development, Going Online, Online, and Retiring. The Industry Facility Investment Logic (detail not shown) is based on relative net present value of a given technology and determines what biorefineries are initiated. The stock of online biorefineries determines what Production Capacity (units of annual volume of biofuel production potential) is available for Industry Capacity Utilization (units of percent) for biofuels production.

DOI: 10.1002/sdr

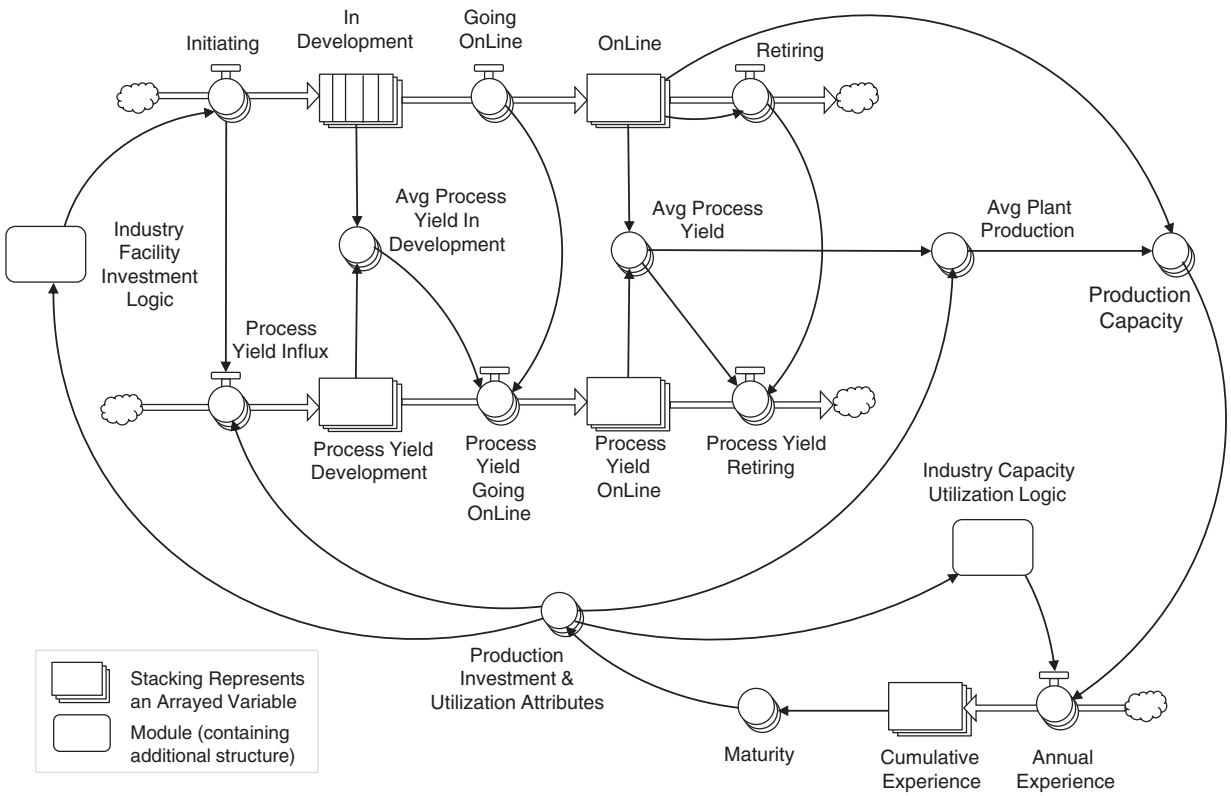

Fig. 1. Partial stock and flow diagram of the biomass learning model, showing biorefinery facility chain and coincident flow of process yield and key feedbacks to investment, production, and utilization

The flow in the middle shows process yield (in units of volume of biofuel per weight of feedstock) contemporaneous with the biorefinery stock, accounting for process yield improvement with technological change over time. Process Yield Development and Process Yield Online stocks parallel biorefinery stocks align the accounting. This enables the appropriate process yield for Average Plant Production (units of annual volume of biofuel possible per plant) at any given time to be calculated for use in the Output Capacity calculation.

The flow at the bottom tracks the stock of Cumulative Experience, measured for the commercial scale in units of volume of biofuel production over all time. This is based on Production Capacity and Industry Capacity Utilization Logic (detail not shown), which includes price–demand feedback. Cumulative industrial experience determines Maturity, which determines the Production, Investment, and Utilization Attributes. The Production, Investment, and Utilization Attributes include capital cost, risk premium,

DOI: 10.1002/sdr

access to debt financing, feedstock throughput, process yield, and feedstock throughput capacity. These feed back to the Industry Facility Investment Logic, Process Yield Stock, Average Plant Production, and Industry Capacity Utilization Logic to complete the reinforcing loop based on the learning curve concept.

A key dynamic in the biomass learning model is the market competition among different technology pathways. A causal loop diagram (Figure 2) summarizes the reinforcing feedback shown in Figure 1, for the competition between two biorefinery technologies. This reinforcing feedback tends to lead toward market dominance of a single technology pathway in the model results, exhibiting path dependence in the system. A technology may outcompete others—due to superior mature techno-economics, higher learning rates, greater initial maturity, or all of these—entering a reinforcing feedback that culminates in market dominance. A technology that attracts more initial investment in biorefineries will then have more fuel production, with associated learning advances. This increase in maturity, and the associated improvements in cost and performance, raises the attractiveness of future investment, for which pathways are assumed to compete. Accordingly, the

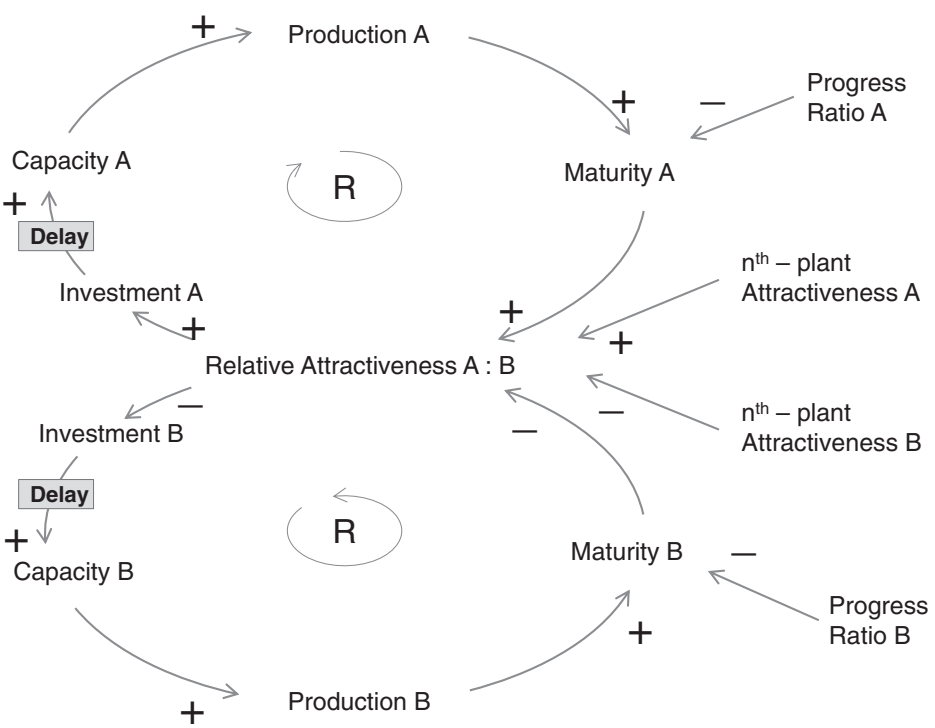

Fig. 2. Causal loop diagram summarizing the effect on relative investment attractiveness of the reinforcing learning feedback loop in the biomass learning model. Source: Vimmerstedt *et al.* (2015)

DOI: 10.1002/sdr

Table 1. Baseline conditions for three technology pathways

Attribute	Technology		
	A	B	C
Initial pilot-scale maturity (0–1 scale)	0.1	0.5	0.85
Pilot-scale operations planned	Yes	Yes	No
Initial demo-scale maturity (0–1 scale)	0	0.5	0.75
Demo-scale operations planned	Yes	Yes	No
n^{th} plant process yield (gal/short ton)	100	90	66
n^{th} plant capital cost (million USD)	30	30	40

reinforcing feedback can lead to complete or partial market dominance: all pathways tend not to succeed equally apart from carefully tuned scenarios.

Baseline model behavior captures competition between three different technology pathways. In the baseline conditions, the technologies are set up as shown in Table 1. The situation in the baseline conditions is such that one technology (Technology C) is close to commercialization, but expensive and with poor process yields. Technology A, on the other hand, is very early in development but has extremely favorable n^{th} (mature) plant capital cost and yield characteristics. Technology B is well into pre-commercial development, with favorable *n*th plant capital costs and process yields that are lower than Technology A, but better than Technology C. Without incentives, none of the technologies represented are able to generate a positive net present value (NPV) under baseline conditions. Incentives, in the form of capital cost subsidies, loan guarantees, and point of production product subsidies, are available to each technology pathway. "Startup" subsidies are set to expire after the first billion gallons of cumulative output for the industry, and "background" subsidies for loan guarantees and capital cost subsidies expire in the year 2022.

Baseline model results are shown in Figure 3. These results show a phased build-out of the different technologies, with Technology A eventually exerting market dominance. Spikes in NPV reflect expiration of startup and background incentives.

The sensitivity analysis in this study assesses the influence of progress ratios values, which contribute to technology maturity, of the three competing pathways in the biomass learning model. The resulting sensitivity analysis will aid in understating how progress ratios, in the context of the learning mechanism in the model, affect the relative competitiveness of technology pathways.

DOI: 10.1002/sdr

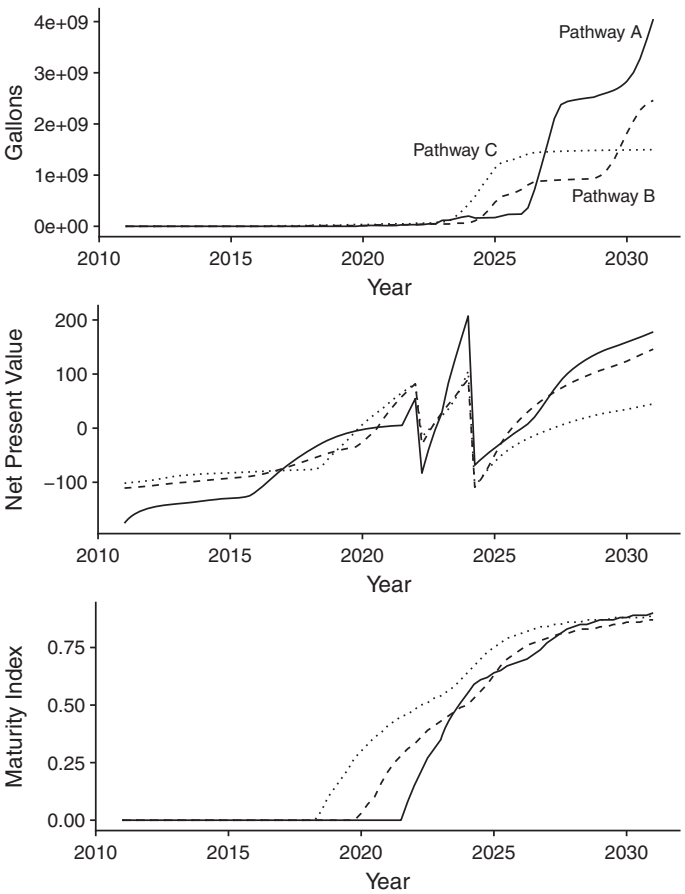

Fig. 3. Biomass learning model simulation results, showing baseline conditions for this study

Methods

The application of Sobol's method to the biomass learning model involved selecting and defining the model factors of interest, output metrics, sampling method, sensitivity indices, uncertainty estimation method, and output function. This section describes the factors of interest in the Learning Model, explains Sobol sensitivity indices, and details the methods used to apply Sobol's method to the biomass learning model.

Biomass learning model factors

Sensitivity analysis enables systematic exploration of the relative importance of various factors in controlling the dynamics of the reinforcing learning feedback loop in the biomass learning model. The term "factors" is used to describe the inputs that were varied in the sensitivity analysis. The biomass

DOI: 10.1002/sdr

learning model analysis evaluates nine factors, each a combination of the progress ratio for a technology pathway (A, B, and C) and an industrial stage (pilot, demonstration, and commercial). For example, the progress ratio for pathway A in the demonstration phase is one factor in the analysis, named *Demo.A*. The progress ratios (Argote, 1999) represent the expectation that costs will decrease as the industry grows and matures and are expressed as a percentage decrease in cost. Values in the range of 0.65–0.90 are used based on historical analogs to the development of the cellulosic biofuels industry (McCurdy *et al.*, 2009).

The biomass learning model produces several output measures that could be used as output metrics for sensitivity analysis, such as estimated costs to the government budget of the available incentives, technological maturity level, and biofuel production. The model output used in this analysis is the total biofuel production (in gallons per year) from all three pathways, as it represents the production of the biofuels system as a whole. Production output for the year 2030 is used. This metric could be useful in assessing the potential for meeting volumetric biofuel policy goals, such as the Renewable Fuel Standard (U.S. Congress, 2005).

Sobol's method

The goal of sensitivity analyses is to quantify the relative importance of input factors in determining a model's output (Saltelli, 2002). In particular, variance-based methods aim to quantify how variance in model inputs can explain variance in model outputs.

Variance-based methods result in calculated sensitivity indices, including first-order, second-order, and total effects indices. In this analysis, we use "order" in the mathematical sense to indicate the number of variables, and not to refer to the order of a delay. The first-order index represents the contribution of a single input factor to the variance in the model output (Saltelli *et al.*, 2008). The second-order index explains the interaction effect of two factors on the model output that cannot be expressed as the sum of their first-order effects. For example, under a certain combination of input values a model may exhibit unique behavior that cannot be explained solely by first-order effects (Saltelli *et al.*, 2008). A model is said to be "non-additive" in the presence of interaction effects, meaning the sum of all first-order effects does not fully capture the variance in model output. Lastly, the total effects index quantifies the total contribution of an input factor to output variance, including the first- and all higher-order effects. Sensitivity indices are represented as a number between 0 and 1.

For this analysis, we implement Sobol's method (Sobol, 1990) to calculate the first-order, second-order, and total effects indices for the progress ratio inputs in the biomass learning model. This paper refers to the key equations used in Sobol's method; readers may refer to Saltelli *et al.* (2008, 2010) for a

DOI: 10.1002/sdr

more comprehensive derivation of the resulting equations. Eq. (3) shows the calculation for the first-order sensitivity index for a factor *i*, where $V(Y)$ represents the unconditional variance of the model output, and V_i represents the conditional variance due to factor *i*. The conditional variance is expressed as $V[E(Y \mid X_i)]$, where $E(Y \mid X_i)$ is the expected value of the output Y keeping X_i fixed, averaged over all possible values of non-X_i factors. The variance of $E(Y \mid X_i)$ is then calculated across all values of X_i (Saltelli *et al.*, 2008). The sensitivity index S_i, then, represents the fractional contribution of the conditional variance due to factor *i* to the unconditional variance of the model. Similarly, Eq. (4) shows the calculation for the second-order sensitivity index for the interaction of factors *i* and *j*:

$$S_i = \frac{V_i}{V(Y)} \tag{3}$$

$$S_{ij} = \frac{V_{ij}}{V(Y)} \tag{4}$$

The sum of all partial variances equals the unconditional variance (Eq. (5)), leading to the relationship of sensitivity indices shown in Eq. (6), which states that all first- and higher-order indices should sum to one. For a purely additive model (i.e. one with no interactions), all higher-order indices equal zero and the sum of only the first-order indices equals one:

$$\sum_i V_i + \sum_i \sum_{j>i} V_{ij} + \ldots V_{12\ldots k} = V(Y) \tag{5}$$

$$\sum_i S_i + \sum_i \sum_{j>i} S_{ij} + \ldots S_{12\ldots k} = 1 \tag{6}$$

In addition to the first- and second-order indices, Sobol's method also estimates the total effects index. The total effects index is implicit in Sobol's method, but was formally introduced in Homma and Saltelli (1996). The total effects index, S_{Ti}, represents the total contribution to model variance of a factor, including the first-order effect and higher-order interactions. Eq. (7) gives an example of the summation of terms for the total effects index of factor X_1 for a three-factor model (Saltelli *et al.*, 2008). For a model with *k* factors, 2^{k-1} terms would have be calculated to compute S_{Ti} by adding all first- and higher-order terms. The Sobol method provides an alternative calculation for the total effects index at the same computational cost as first-order indices. Eq. (8) shows the formulation of the total effects index, where $E(Y \mid X_{\sim i})$ is the expected value of Y fixing all factors except X_i, averaged over all values of X_i:

$$S_{Ti} = S_1 + S_{12} + S_{13} + S_{123} \tag{7}$$

DOI: 10.1002/sdr

$$S_{Ti} = 1 - \frac{V[E(Y|X_{\sim i})]}{V(Y)} \tag{8}$$

The total effects index reveals non-additivity in a model when the index value is greater than the first-order sensitivity index for a given factor, signaling the existence of non-zero higher-order indices. The total effects index can also be used to determine an influential, or non-influential, factor. A total effects index of zero means that a factor can take on any value without significantly affecting the model output.

Sampling method

To compute the estimates of the sensitivity indices, two independent sample matrices of model input values are required (Saltelli, 2002) that cover the input parameter space. The matrices, referred to as A and B, are each of size $N \times k$, where N is the base sample size and k is the number of factors. Input factors are assumed to be independent of one another and, as recommended by Saltelli *et al.* (2008), quasi-random sequences are used to generate the input values for the sample matrices (we do not assume probability distributions for the input values). Quasi-random sequences have fewer clusters and gaps in sample values compared to purely random sequences, which results in a better spread of input values. R Statistical Programming Language was used to design the sampling process (see Supporting Information). Each row in the matrices represents the factor values for a single model run. For this study, the factor values represent the progress ratios for the three technology pathways in each stage of industrial development. Figure 4 shows example matrices for an analysis with three factors and a sample size of four.

Using matrices A and B, k additional matrices are formed by taking every column from A except the ith column, which has been substituted from B. We refer to this matrix as $A_B^{(i)}$. Similarly, an additional set of k matrices, referred to as $B_A^{(i)}$, is formed by taking every column of B except the ith, which has been substituted from A. These matrices are used to produce model output values where all factor values have changed, except those of the ith factor, allowing the computation of variance attributed to single factors. Example sets of $A_B^{(i)}$ and $B_A^{(i)}$ matrices are represented in Figure 5.

$$A = \begin{bmatrix} a_{11} & a_{12} & a_{13} \\ a_{21} & a_{22} & a_{23} \\ a_{31} & a_{32} & a_{33} \\ a_{41} & a_{42} & a_{43} \end{bmatrix} \qquad B = \begin{bmatrix} b_{11} & b_{12} & b_{13} \\ b_{21} & b_{22} & b_{23} \\ b_{31} & b_{32} & b_{33} \\ b_{41} & b_{42} & b_{43} \end{bmatrix}$$

Fig. 4. Independent matrices, A and B, where *a* and *b* represent values from quasi-random sequences

DOI: 10.1002/sdr

Fig. 5. The set of $A_B^{(i)}$ matrices (left), and the set of $B_A^{(i)}$ matrices (right)

$$A_B^{(1)} = \begin{bmatrix} b_{11} & a_{12} & a_{13} \\ b_{21} & a_{22} & a_{23} \\ b_{31} & a_{32} & a_{33} \\ b_{41} & a_{42} & a_{43} \end{bmatrix} \qquad B_A^{(1)} = \begin{bmatrix} a_{11} & b_{12} & b_{13} \\ a_{21} & b_{22} & b_{23} \\ a_{31} & b_{32} & b_{33} \\ a_{41} & b_{42} & b_{43} \end{bmatrix}$$

$$A_B^{(2)} = \begin{bmatrix} a_{11} & b_{12} & a_{13} \\ a_{21} & b_{22} & a_{23} \\ a_{31} & b_{32} & a_{33} \\ a_{41} & b_{42} & a_{43} \end{bmatrix} \qquad B_A^{(2)} = \begin{bmatrix} b_{11} & a_{12} & b_{13} \\ b_{21} & a_{22} & b_{23} \\ b_{31} & a_{32} & b_{33} \\ b_{41} & a_{42} & b_{43} \end{bmatrix}$$

$$A_B^{(3)} = \begin{bmatrix} a_{11} & a_{12} & b_{13} \\ a_{21} & a_{22} & b_{23} \\ a_{31} & a_{32} & b_{33} \\ a_{41} & a_{42} & b_{43} \end{bmatrix} \qquad B_A^{(3)} = \begin{bmatrix} b_{11} & b_{12} & a_{13} \\ b_{21} & b_{22} & a_{23} \\ b_{31} & b_{32} & a_{33} \\ b_{41} & b_{42} & a_{43} \end{bmatrix}$$

The method calls for $N(2k+2)$ model runs to compute the full set of first-order, second-order, and total effects sensitivity indices.

The resulting $2k+2$ vectors of model outputs corresponding to the input values in each matrix row are used to compute the sensitivity indices described in the next section. For the subsequent sections, let $f(A)_j$ be the jth value in the output vector of size N, corresponding to the model inputs from matrix A, with similar notation for the remaining matrices. Readers may refer to the R code provided in the Supporting Information to review how the sampling matrices were implemented in this analysis.

Table 2. Sensitivity estimate calculations analyzed from various sources

	Method 1 Sobol (1990), Homma and Saltelli (1996)	Method 2 Homma and Saltelli (1996)	Method 3 Saltelli *et al.* (2010)
f_0^2	$\left(\frac{1}{N}\sum_{j=1}^{N} f(A)_j\right)^2$	$\frac{1}{N}\sum_{j=1}^{N} f(A)_j f(B)_j$	(Same as Method 2)
S_i	$\frac{\frac{1}{N}\sum_{j=1}^{N} f(A)_j f\left(B_A^{(i)}\right)_j - f_0^2}{V(Y)}$	$\frac{\frac{1}{N}\sum_{j=1}^{N} f(A)_j f\left(B_A^{(i)}\right)_j - f_0^2}{V(Y)}$	$\frac{\frac{1}{N}\sum_{j=1}^{N} f(B)_j \left(f\left(A_B^{(i)}\right)_j - f(A)_j\right)}{V(Y)}$
S_{Ti}	$1 - \frac{\frac{1}{N-1}\sum_{j=1}^{N} f(B)_j f\left(B_A^{(i)}\right)_j - f_0^2}{V(Y)}$	(Same as Method 1)	$\frac{\frac{1}{2N}\sum_{j=1}^{N} \left(f(A)_j - f\left(A_B^{(i)}\right)_j\right)^2}{V(Y)}$

DOI: 10.1002/sdr

Sensitivity index estimates

Various methods have been proposed to calculate the first-order and total effects sensitivity indices described above, which aim to improve upon the formulations presented in Sobol (1990) (Saltelli (2002), and Saltelli *et al.* (2008, 2010)). We analyzed three different methods based on recent literature to understand the advantages and restrictions of each; the three methods exhibit a progression in method improvement and are summarized in Table 2.

The initial sensitivity index computations explored in this analysis, referred to as Method 1, were proposed in Saltelli *et al.* (2008); the calculations are based on the original formulations presented in Sobol (1990), with the addition of the total effects calculation introduced in Homma and Saltelli (1996). The second method analyzed, Method 2, incorporates improvements proposed by Homma and Saltelli (1996). The new calculation for f_0^2 in Method 2 aims to increase the accuracy of the first-order estimates by using output from both the A and B matrices. Finally, Method 3 represents the calculations suggested in Saltelli *et al.* (2010), which includes an adjustment to the calculation for V_i from previous improvements based on Saltelli (2002), Sobol *et al.* (2007), and Jansen (1999).

To assess methods, we analyzed differences in estimate accuracy and estimate values for S_i and S_{Ti}. Figure 6 shows the comparison of Methods 1 and 2, which confirms the increased accuracy of first-order estimates in Method 2. As seen in the upper left chart, the 95 percent bootstrap confidence interval (BCI) (see "Uncertainty of sensitivity estimates") for S_i is lower for Method 2 than for Method 1, with no significant effect on the values of the estimates (shown in the upper right chart). The accuracy and estimate values for the total effects indices are consistent across these methods, as they employ the same equation to calculate total effects.

The comparison of accuracy and estimated values for Methods 2 and 3 is shown in Figure 7. These results indicate the improvement in total effects estimate accuracy obtained from Method 3, with no appreciable effect on the estimate values. The analysis of methods resulted in the final equations used in this study to calculate sensitivity index estimates, which are from Method 3 and summarized in Table 3.

Sobol suggests that the accuracy of the estimates described above can decrease with large values of f_0 (Sobol, 1990). Because the output analyzed in the biomass learning model is of the order of billions of gallons, numerical errors may lead to inaccurate estimate calculations. To improve the numeric round-off accuracy, Sobol proposes to center the model output using an approximate estimate of the mean, c_0, and substitute $f(x)$ with $f(x) - c_0$ (Sobol, 1990). We confirmed that this approach improved estimate accuracy and centered all output in this analysis; the Appendix includes a comparison of centered and non-centered output for Method 1.

DOI: 10.1002/sdr

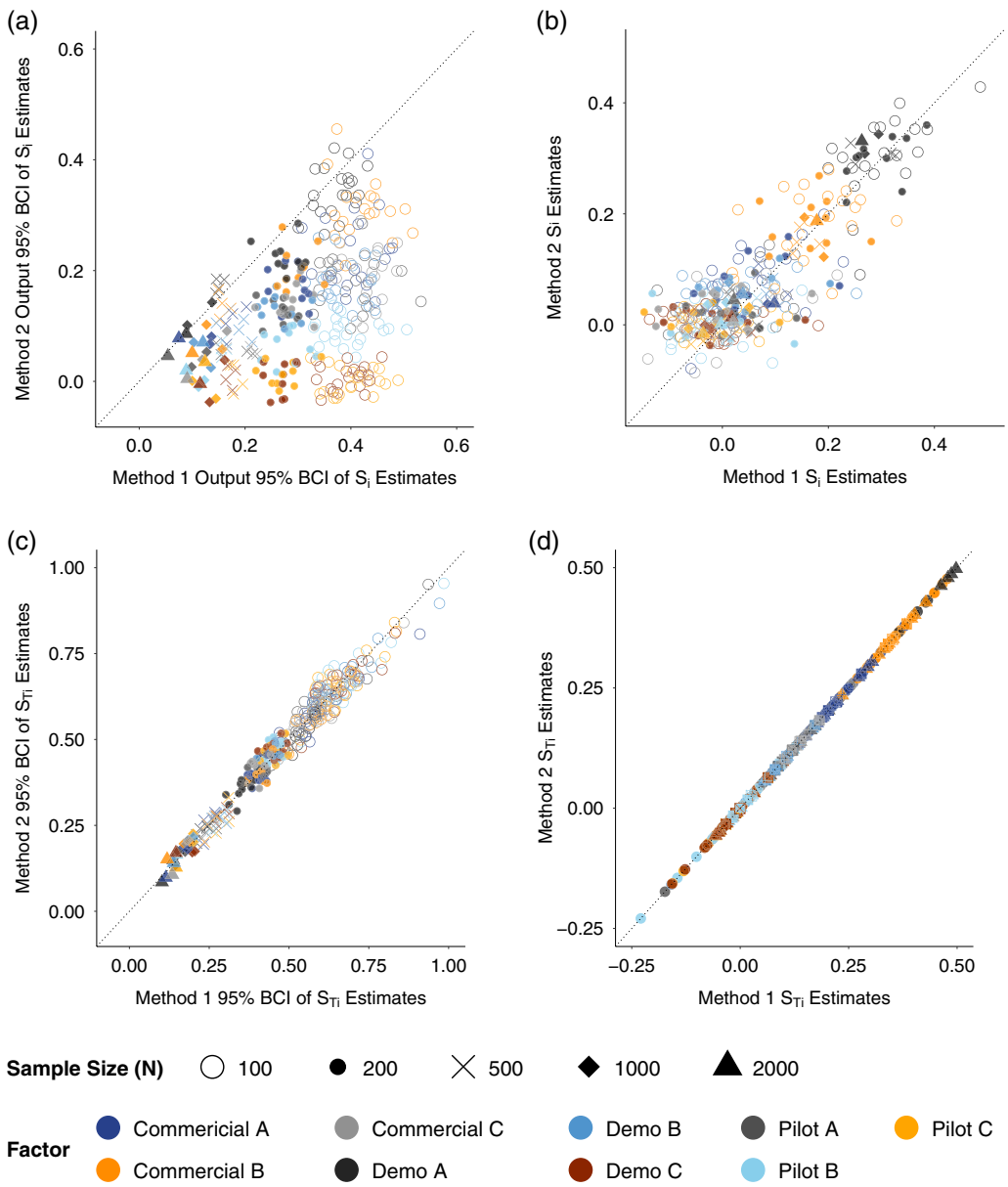

Fig. 6. Comparison of Method 1 (on the *x*-axis) and Method 2 (on the *y*-axis): (a) 95 percent BCI width for S_i; (b) S_i estimates; (c) 95 percent BCI width for S_{T_i}; (d) S_{T_i} estimates. [Color figure can be viewed at wileyonlinelibrary.com]

DOI: 10.1002/sdr

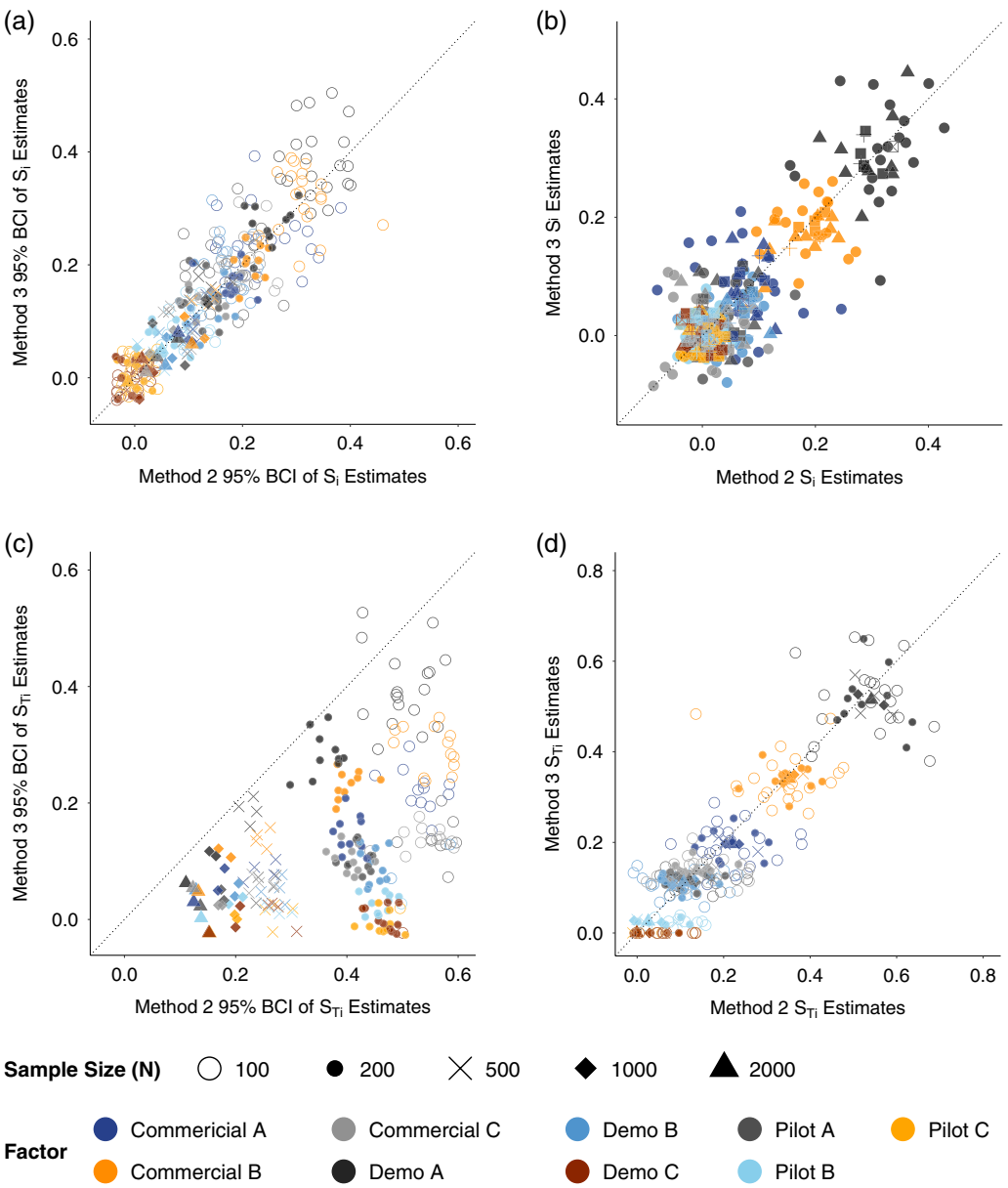

Fig. 7. Comparison of Method 2 (on the *x*-axis) and Method 3 (on the *y*-axis): (a) 95 percent BCI width for S_i; (b) S_i estimates; (c) 95 percent BCI width for S_{T_i}; (d) S_{T_i} estimates. [Color figure can be viewed at wileyonlinelibrary.com]

DOI: 10.1002/sdr

Table 3. Estimate calculations used for biomass learning model sensitivity analysis

Estimate	Estimate equation
f_0^2	$\frac{1}{N}\sum_{j=1}^{N} f(A)_j f(B)_j$
$V(Y)$	$\sum_{j=1}^{N} f(A)_j^2 - f_0^2$
S_i	$\frac{\frac{1}{N}\sum_{j=1}^{N} f(B)_j \left(f\left(A_B^{(i)}\right)_j - f(A)_j\right)}{V(Y)}$
S_{Ti}	$\frac{\frac{1}{2N}\sum_{j=1}^{N} \left(f(A)_j - f\left(A_B^{(i)}\right)_j\right)^2}{V(Y)}$

As previously described, Sobol's method can also be implemented for the estimation of higher-order sensitivity indices. The sampling method used in this research allows for the estimation of second-order indices (Saltelli, 2002); Eq. (9) shows the estimate calculation used in this analysis:

$$S_{ij} = \frac{\frac{1}{N}\sum_{w=1}^{N} f\left(A_B^{(i)}\right)_w f\left(B_A^{(j)}\right)_w - V_i - V_j}{V(Y)} \tag{9}$$

The summation term in Eq. (9) represents V_{ij}^c, which is the closed partial variance for factors i and j. The closed index includes the first-order effects of the two factors and the interaction term: for example, $V_{12}^c = V_1 + V_2 + V_{12}$. In order to obtain the interaction effect estimate, the first-order effects are subtracted from the closed index (Saltelli, 2002).

Uncertainty of sensitivity indices

A major goal of this research is to understand the uncertainty of the sensitivity index estimates. In this section we compare two methods: bootstrapping and a numeric calculation presented in Saltelli *et al*. (2008).

The calculation included in Saltelli *et al*. (2008), shown in Eq. (10), computes the error of V_i and was modified for this analysis for the estimate calculations used in Table 3. The modified equations are included in the Appendix:

$$\frac{1.96}{\sqrt{N}} \sqrt{\frac{1}{N}\sum_{j=1}^{N} \left(f(A)_j f\left(B_A^{(i)}\right)\right)^2 - \left(\frac{1}{N}\sum_{j=1}^{N} f(A)_j f\left(B_A^{(i)}\right)\right)^2} \tag{10}$$

Bootstrap resampling was also used to calculate the confidence intervals for the first-order, second-order, and total effects sensitivity indices (Efron and Tibshirani, 1998). We resampled the $N(2k+2)$ model evaluations 1000

DOI: 10.1002/sdr

times with replacement, calculating the sensitivity indices with each resample. The 1000 resamples yield a bootstrap estimate of the sampling distribution for each sensitivity index. We then used the percentile method (Archer *et al.*, 1997; Efron and Tibshirani, 1998) to establish the 95 percent BCI from the 2.5 to the 97.5 percentiles of the bootstrap distribution. The bootstrap is a resampling method that relies on random sampling with replacement. Resampling means selecting new samples that are subsets of results. "With replacement" means that each sample draws from the same set of results, rather than having results that are part of one sample become unavailable to subsequent samples. Bootstrapping may be applied to produce estimates of statistical properties of interest such as the mean and variance by sampling from an approximate distribution, such as the empirical distribution function of the observed data (Efron and Tibshirani, 1998). Because the distribution is taken from the observed data, hypothesis tests that are based on bootstrapped estimators are nonparametric, meaning that we are not making assumptions about the statistical distribution of the observations.

We compared the uncertainty estimates obtained from our results for both methods. For the first-order index, the BCI and numeric calculation produce congruent uncertainty estimates. In contrast, the numeric calculation yields higher uncertainty for the total effects index, especially when the factors have high index estimates. Even with the inconsistency in the total effects uncertainty, these results give us confidence that the numeric calculation approach can be used as a guide for sample size selection in order to obtain a desired accuracy, instead of using bootstrap resampling.

Results

We calculated the sensitivity index estimates for the biomass learning model, using the calculations described under "Sensitivity index estimates",

Table 4. First-order sensitivity indices and 95% BCIs

Factor i	S_i estimate	Bootstrap average	95% BCI	
Demo.A	0.305	0.305	0.265	0.344
Commercial.B	0.179	0.179	0.145	0.213
Commercial.A	0.075	0.075	0.047	0.101
Demo.B	0.054	0.054	0.035	0.075
Pilot.A	0.036	0.035	0.015	0.055
Commercial.C	0.013	0.014	−0.009	0.035
Pilot.B	0.005	0.005	−0.005	0.016
Pilot.C	0.000	0.000	−0.001	0.001
Demo.C	0.000	0.000	0.000	0.000

DOI: 10.1002/sdr

Table 5. Total effects indices and 95% BCIs

Factor i	S_{T_i} estimate	Bootstrap average	95% BCI	
Demo.A	0.523	0.523	0.478	0.571
Commercial.B	0.346	0.346	0.312	0.381
Commercial.A	0.200	0.201	0.178	0.226
Commercial.C	0.140	0.140	0.126	0.155
Pilot.A	0.117	0.118	0.103	0.134
Demo.B	0.113	0.114	0.101	0.129
Pilot.B	0.026	0.026	0.022	0.030
Pilot.C	0.000	0.000	0.000	0.000
Demo.C	0.000	0.000	0.000	0.000

above. The analysis consisted of a sample size of $N = 2000$, requiring 40,000 runs (or $N(2k+2)$).

Estimates

The calculated first-order and total effects indices for the biomass learning model factors are displayed in Tables 4 and 5, respectively. Referring to the results in those tables, *Demonstration A (Demo.A)* is shown to be the most influential factor in the model. From the interpretation of S_i given in "Sobol's method", we could reduce the model output variation by a factor of 0.305, on average, by fixing the input values for the *Demo.A* factor. In contrast, the variable *Demonstration C (Demo.C)* is the least influential. This result is validated from the biomass learning model, which does not include any plants at the demonstration scale for technology pathway C; this factor is not influential under our model conditions. The results in Table 5 show that *Pilot C* is also non-influential, with a lower BCI bound for S_{Ti} equal to zero. As previously mentioned, the total effects index can be used to identify a non-influential variable since the estimate also includes interaction effects, which are not apparent when looking only at S_i.

We can also gain insight into the impact of the various industrial stages by examining the total effect index estimates. Besides the factor *Demo.A*, the three factors with the highest S_{Ti} estimates are the commercial progress ratios. For the biomass learning model, the learning rates of the commercial stage have greater influence on total biofuel production than pilot and demonstration stage learning rates.

Table 6. Second-order indices and 95% BCIs

Parameter i–j	S_{ij} estimate	Bootstrap average	95% BCI	
D.A–C.A	0.075	0.076	0.035	0.119
C.B–C.C	0.048	0.048	0.017	0.083

DOI: 10.1002/sdr

Table 6 lists the significant interaction effects of factor pairs from the analysis, *Demonstration A–Commercial A* (*D.A–C.A*) and *Commercial B–Commercial C* (*C.B–C.C*). The most influential effect, *D.A–C.A*, can be attributed to the tendency for technology A to dominate the market. The interaction term indicates that if both Demonstration and Commercial progress ratios for pathway A are low (i.e. fast learning rates), the technology will yield higher production outputs than would be explained by the increase in output from the two factors independently. The other significant second-order effect, *C.B–C.C*, highlights the competition in the market. If both *Commercial B* and *Commercial C* experience fast learning, this acts as a balance for pathway A, which will then be less likely to yield high output. Note that in Table 4 *Commercial C* does not have a significant first-order effect, while the total effects estimate is significant; only in combination with *Commercial B*, or other factors, will the variance of *Commercial C* significantly affect model output. This *C.B–C.C* interaction effect further illustrates the greater influence of the commercial scale over pilot and demonstration.

The presence of significant interaction effects, in combination with further observation of the estimates in Tables 4 and 5, clearly reveals that our model is non-additive, as was to be expected. The sum of S_i and S_{Ti} should both equal one in an additive model, which is not true of our calculated estimates. The addition of the second-order interaction terms accounts for further model variance, but the results suggest the model has possible higher-order interactions. As referenced in Eq. (6), the sum of all first-order effects and higher-order interactions of a model should equal one. For our model, the sum of all first-order effects is 0.667.

Conclusion

This study illustrates the application of a statistically rigorous sensitivity analysis to a system dynamics model. Although this study focused on an extract of the much larger BSM, the approach presented is applicable to the sensitivity analysis of much larger models. The upper limit of model factors to analyze is dependent on computing resources available. Using Sobol's method, we are able to characterize the behavior of the biomass learning model across the factors' ranges as well as identify the most influential factors and interactions among factors. The ability to quantitatively identify interaction effects distinguishes this methodology from those described in the Introduction. This approach is particularly well suited for gaining insights from system dynamic models such as the biomass learning model, where the model is non-additive, has a number of potential interactions, and is too complex to readily assess all combinations of factors across their ranges.

Our approach generates $N(2k+2)$ distinct model runs, which requires considerable computational resources. The width of the bootstrapped

DOI: 10.1002/sdr

confidence intervals for both S_i and S_{T_i} follows an exponential decay function when plotted against N, for $N = 0$–4000. The slope of this function reaches approximately one at $N = 2000$, which suggests that a sample size of $N = 2000$ has adequate statistical power for both the total and the first-order effects. Application of this method to other models should include similar analysis of confidence intervals at varying sample sizes, and the maximum sample size may be constrained by the available computational resources.

A combination of calculation methods from recent literature resulted in the best accuracy. Saltelli *et al.*'s (2010) proposed method to estimate total effects and Saltelli *et al.*'s (2008) proposed method to estimate first-order effects produced the most accurate results. Although we anticipate that this finding is generalizable, analysts applying this method to their own models may wish to perform bootstrapped uncertainty analysis to confirm method accuracy.

The analysis presented here identifies the most influential and interactive progress ratios. These are consistent with the model formulation and previous analysis using traditional system dynamics approaches, but this analysis provides quantitative confirmation of those qualitative findings—confirmation that may be particularly helpful when working with large system dynamics models.

We provide annotated R code in the online supplement (Supporting Information Appendix S1) and access to the full STELLA file for the biomass learning model (https://github.com/NREL/bsm-learning) to facilitate application of the method to other models. This method is recommended for an analysis involving 20 or fewer factors, due to its computational intensity (Saltelli and Saisana, 2007). A total effects analysis may be possible within this limit for small models, but for larger numbers of factors an elementary effects analysis may be used to screen out factors before performing a total effects analysis (Morris, 1991; Alam *et al.*, 2004).

By applying variance-based sensitivity analysis techniques to a moderate-sized published STELLA model, we establish methods that are applied to the full BSM in related work (Inman *et al.*, 2018) and illustrate that the method provides insights that would be more difficult to obtain using traditional systems analysis techniques.

Biographies

Paige Jadun is an energy systems modeler at NREL, focusing on sustainable transportation, hydrogen production and utilization, and electrification.

Laura J. Vimmerstedt has over ten years of experience managing major transportation and energy analysis projects at NREL. Her technical expertise includes biofuels supply chain modeling and analysis.

DOI: 10.1002/sdr

Brian W. Bush has twenty five years of experience with infrastructure, energy, and transportation modeling, simulation, and analysis.

Daniel Inman, a PhD soil scientist, has over ten years of experience in bioenergy feedstocks, modeling, and advanced statistics.

Steve Peterson is an independent consultant and a Senior Lecturer at the Thayer School of Engineering at Dartmouth College. Steve has been involved in the teaching and application of dynamic modeling approaches since the early 1980s.

References

Alam FM, McNaught KR, Ringrose TJ. 2004. Using Morris' randomized OAT design as a factor screening method for developing simulation metamodels. In *Proceedings of the 2004 Winter Simulation Conference, IEEE*, pp. 930–938.

Archer GEB, Saltelli A, Sobol IM. 1997. Sensitivity measures, ANOVA-like techniques and the use of bootstrap. *Journal of Statistical Computation and Simulation* **58**: 99–120.

Argote L. 1999. *Oganizational Learning: Creating, Retaining, and Transferring Knowledge*. Springer: Berlin.

Bier A. 2011. Sensitivity analysis techniques for system dynamics models of human behavior. In *29th International Conference of the Systems Dynamics Society*, Washington, DC. Available: https://www.systemdynamics.org/assets/conferences/2011/proceed/papers/P1112.pdf [30 May 2018].

Efron B, Tibshirani RJ. 1998. *An Introduction to the Bootstrap*. Chapman & Hall: London, U.K.

Eker S, Slinger J, van Daalen E, Yücel G. 2014. Sensitivity analysis of graphical functions. *System Dynamics Review* **30**: 186–205.

Ford A, Flynn H. 2005. Statistical screening of systems dynamics models. *System Dynamics Review* **21**: 273–303.

Hekimoğlu M, Barlas Y. 2016. Sensitivity analysis for models with multiple behavior modes: A method based on behavior pattern measures. *System Dynamics Review* **32**: 332–362.

Homma T, Saltelli A. 1996. Importance measures in global sensitivity analysis of nonlinear models. *Reliability Engineering and System Safety* **52**: 1–17.

Inman D, Vimmerstedt LJ, Bush B, Stright D, Peterson S. 2018. Application of variance-based sensitivity analysis to a large system dynamics model. arXiv. doi: arXiv:1803.10722 [stat.AP].

isee systems. 2014. STELLA: systems thinking for education and research software. Available: http://www.iseesystems.com/softwares/Education/StellaSoftware [26 October 2010].

Jalili Y, Ford DN. 2016. Quantifying the impacts of rework, schedule pressure, and ripple effect loops on project schedule performance. *System Dynamics Review* **32**: 82–96.

DOI: 10.1002/sdr

Jansen M. 1999. Analysis of variance designs for model output. *Computer Physics Communications* **117**: 35–43.

Kleijnen JPC. 1995. Sensitivity analysis and optimization of system dynamics models: Regression analysis and statistical design of experiments. *System Dynamics Review* **11**: 275–288.

Lin Y, Newes E, Bush B, Peterson S, Stright D. 2013. Biomass scenario model documentation: data and references. Technical Report NREL/TP- 6A20-57831. National Renewable Energy Laboratory. Golden, CO. Available: http://www.osti.gov/bridge/servlets/purl/1082565/ [30 May 2018].

McCurdy M, Hegazy Y, Norland D, Victor N. 2009. An examination of technology learning method and its applications tailored to industrial technologies for converting lignocellulosic biomass to fuels. SR-6A20-63543. National Renewable Energy Laboratory, Golden, CO.

Morris MD. 1991. Factorial sampling plans for preliminary computational experiments. *Technometrics* **33**(2): 161–174.

Peterson S, Peck C, Stright D, Newes E, Inman D, Vimmerstedt L, Hsu D, Bush B. 2013. An overview of the biomass scenario model. In *31st International Conference of the System Dynamics Society*, Cambridge, MA. Available: http://www.nrel.gov/docs/fy15osti/60172.pdf [30 May 2018].

Pianosi F, Beven K, Freer J, Hall JW, Rougier J, Stephenson DB, Wagener T. 2016. Sensitivity analysis of environmental models: A systematic review with practical workflow. *Environmental Modelling and Software* **79**: 214–232.

Saltelli A. 2002. Making best use of model evaluations to compute sensitivity indices. *Computer Physics Communications* **145**: 280–297.

Saltelli A, Annoni P, Azzini I, Campolongo F, Ratto M, Tarantola S. 2010. Variance based sensitivity analysis of model output: Design and estimator for the total sensitivity index. *Computer Physics Communications* **181**: 259–270.

Saltelli A, Ratto M, Andres T, Campolongo F, Cariboni J, Gatelli D, Saisana M, Tarantola S. 2008. *Global Sensitivity Analysis: The Primer*. Wiley: Hoboken, NJ.

Saltelli A, Saisana M. 2007. Settings and methods for global sensitivity analysis: a short guide. In *Sixth International Congress on Industrial Applied Mathematics (ICIAM07) and GAMM Annual Meeting*, Zürich, 2007. Available: http://onlinelibrary.wiley.com/doi/10.1002/pamm.200700986/abstract [30 May 2018].

Saltelli A, Tarantola S, Campolongo F, Ratto M. 2004. *Sensitivity Analysis in Practice: A Guide to Assessing Scientific Models*. Wiley: Chichester, U.K.

Sobol IM. 1990. Sensitivity estimates for nonlinear mathematical models. *Matematicheskoe Modelirovanie* **2**: 112–118 [in Russian].

Sobol IM. 1993. Sensitivity analysis for nonlinear mathematical models. *Mathematical Modeling and Computational Experiment* **1**: 407–414.

Sobol IM, Tarantola S, Gatelli D, Kucherenko SS, Mauntz W. 2007. Estimating the approximation error when fixing unessential factors in global sensitivity analysis. *Reliability Engineering and System Safety* **92**(7): 957–960.

Sterman JD. 2000. *Business Dynamics: Systems Thinking and Modeling for a Complex World*. McGraw-Hill: New York.

Taylor TRB, Ford DN, Ford A. 2010. Improving model understanding using statistical screening. *System Dynamics Review* **26**: 73–87.

U.S. Congress. 2005. Energy Policy Act of 2005. HR 6: 109th Congress.

DOI: 10.1002/sdr

Vimmerstedt L, Bush B, Peterson S. 2015. Dynamic modeling of learning in emerging energy industries: the example of advanced biofuels in the United States. In *33rd International System Dynamics Conference*, Cambridge, MA.

Walrave B. 2016. Determining intervention thresholds that change output behavior patterns. *System Dynamics Review* **32**: 261–278.

Appendix

Estimate uncertainty

Saltelli *et al.* (2010) presented a numerical calculation for the error of V_i. We modified the equation for the sensitivity index estimate calculations described under "Sensitivity index estimates" in the main text. Eqs. (A.1) and (A.2) show the modified numerical uncertainty equations used for the first-order and total effects estimates, respectively:

$$\frac{1.96}{\sqrt{N}}\sqrt{\frac{1}{N}\sum_{j=1}^{N}\left(f(B)_j\left(f\left(A_B^{(i)}\right)_j - f(A)_j\right)\right)^2 - \left(\frac{1}{N}\sum_{j=1}^{N} f(B)_j\left(f\left(A_B^{(i)}\right)_j - f(A)_j\right)\right)^2} \tag{A.1}$$

$$\frac{1.96}{\sqrt{N}}\sqrt{\frac{1}{N}\sum_{j=1}^{N}\left(f(A)_j - f\left(A_B^{(i)}\right)_j\right)^2 - \left(\frac{1}{N}\sum_{j=1}^{N}\left(f(A)_j - f\left(A_B^{(i)}\right)_j\right)\right)^2} \tag{A.2}$$

Centered output

Figure A1 shows a comparison of using the original and centered output for Method 3 when calculating the first-order and total effects indices. The left plots in Figure A1 show the length of the 95 percent BCI and represent the method accuracy. The centered output clearly produces more accurate estimates, but the actual index estimates are similar, as seen in the right-hand figures. The same trends can be seen for the first-order and total effects indices. The results for Methods 1 and 2 exhibit similar behavior. These results indicate that centering the output increases the accuracy of the estimates, but does not significantly change the estimated values.

DOI: 10.1002/sdr

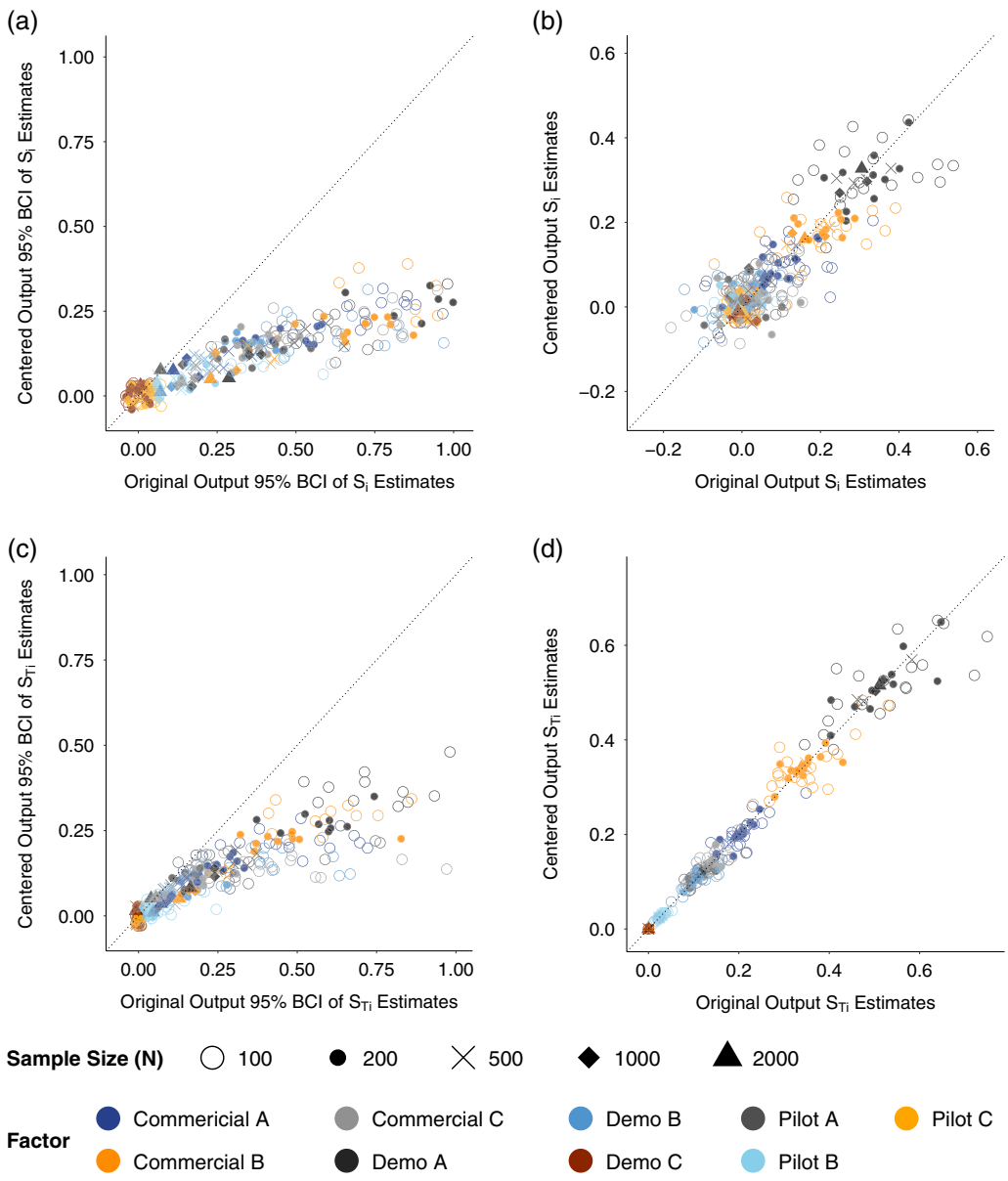

Fig. A1. Comparison of original and centered model output for Method 3; original output is on the *x*-axis, centered is on the *y*-axis: (a) 95 percent BCI width for S_i; (b) S_i estimates; (c) 95 percent BCI width for S_{T_i}; (d) S_{T_i} estimates. [Color figure can be viewed at wileyonlinelibrary.com]

DOI: 10.1002/sdr

Supporting information

Additional supporting information may be found online in the Supporting Information section at the end of the article.

Appendix S1 Model documentation and annotated R code.

DOI: 10.1002/sdr